Cell J
Cell Journal(Yakhteh)
Homepage: https://www.celljournal.org/
Original Article
Vol 25, No 8, August 2023, Pages: 579-590

Co-Culture of Mouse Blastocysts on A Human Recellularized Endometrial Scaffold: An *In Vitro* Model for Future Implantation Studies

Elham Sadeghi, Ph.D., Mojtaba Rezazadeh Valojerdi, Ph.D., Mojdeh Salehnia, Ph.D.*

Department of Anatomy, Faculty of Medical Sciences, Tarbiat Modares University, Tehran, Iran

Abstract

Objective: This study evaluates the interaction of mouse blastocysts as a surrogate embryo on a recellularized endometrial scaffold by seeding human endometrial mesenchymal cells (hEMCs).

Materials and Methods: In this experimental study, prepared decellularized human endometrial tissues were characterized by morphological staining, DNA content analysis, and scanning electron microscopic (SEM) analysis. The scaffolds were subsequently recellularized by hEMCs. After seven days of cultivation, the mouse blastocysts were co-cultured on the recellularized scaffolds for 48 hours. Embryo attachment and implantation within these scaffolds were evaluated at the morphological, ultrastructural, molecular, and hormonal levels.

Results: There was no morphological evidence of cells and nuclei in the decellularized scaffold. DNA content significantly decreased by 89.92% compared to the control group (P<0.05). Both decellularized and native tissues had similar patterns of collagen bundles and elastin fibers, and glycosaminoglycan (GAGs) distribution in the stroma. After recellularization, the hEMCs attached to the scaffold surface and penetrated different parts of these scaffolds. In the co-cultured group, the embryo attached to the surface of the scaffold after 24 hours and penetrated the recellularized endometrial tissue after 48 hours. We observed multi-layered organoid-like structures formed by hEMC proliferation. The relative expressions of epithelial-related genes, *ZO-1* and *COL4A1,* and *SSP1, MMP2,* and *PRL*, as decidualization-related genes, were significantly higher in the recellularized group on day 9 in the presence of the embryo compared to the other groups (P<0.05). Beta human chorionic gonadotropin (β-hCG) and prolactin were statistically increased in the recellularized group on day 9 group (P<0.05).

Conclusion: hEMCs and mouse embryo co-cultured on a decellularized endometrial scaffold provides an alternative model to study embryo implantation and the earlier stage of embryo development.

Keywords: Decellularized Extracellular Matrix, Decidualization, Embryo Implantation, Endometrium, Mesenchymal Stem Cells

Citation: **Sadeghi E, Rezazadeh Valojerdi M, Salehnia M. Co-culture of mouse blastocysts on a human recellularized endometrial scaffold: an in vitro model for future implantation studies. Cell J. 2023; 25(8): 579-590. doi: 10.22074/CELLJ.2023.1989926.1236**

Introduction

In vitro endometrial regeneration could provide a valuable system to study endometrial physiological events such as decidualization and embryo implantation (1-5). Current three-dimensional (3D) culture system models use synthetic and natural bioscaffolds such as collagen and Matrigel to renovate the endometrium (1, 5-7). The major disadvantage of synthetic biomaterials is their different structure and composition in comparison with native tissues (8). Although natural biomaterials support cell adhesion, migration, proliferation and differentiation, their composition varies from batch to batch and they must be characterized prior to use. Decellularized endometrial extracellular matrix (ECM) is the best bioscaffold choice due to its similarity to native tissue components (9-11).

Decellularization involves the removal of cellular components by exposing the tissues to detergents and physical forces, or to various enzymatic solutions in an attempt to create a specific tissue ECM (12, 13). The purpose of decellularization is to preserve tissue structures and ECM components, despite the removal of cell materials.

Successful decellularization of whole uteri and endometrial fragments have been reported in several mammalian species (14-20). Recently, we developed a combined protocol for the decellularization of human endometrial tissue fragments where the amount of ECM component did not change in the decellularized tissues. Moreover, both porosity and ECM fibre in the created scaffold were similar to the intact tissue (21).

In another approach, endometrial cell-free scaffolds

Received: 18/February/2023, Revised: 25/April/2023, Accepted: 25/June/2023
***Corresponding Address: P.O.Box: 14115-111, Department of Anatomy, Faculty of Medical Sciences Tarbiat Modares University, Tehran, Iran**
Email: salehnim@modares.ac.ir

Royan Institute
Cell Journal (Yakhteh)

are recellularized using human stromal and epithelial side populations of stem cells, primary endometrial cells, and bone marrow mesenchymal stem cells (9, 18, 22, 23).

Attempts have been made to replicate normal conditions by utilizing endometrial and myometrial cells in collagen, matrigel and other types of biomaterials. The functional characteristics of these reconstructed structures were evaluated through embryo implantation (2, 24-27).

Several embryo implantation models have been generated since the first laboratory model of mammalian implantation was proposed by Glenister in 1961 (7, 28, 29). The single-layer model focuses on pre-implantation interactions between epithelial cells and human embryos (30). Embryos co-cultured with endometrial stromal cells comprised the second step of embryo implantation, and the effect of blastocyst-derived factors and their penetration within the endometrial epithelium were evaluated (31). In the most complex model, the initial to final stages of embryo implantation were studied in a 3D culture system where researchers sought to evaluate paracrine signals, cell-cell, cell-ECM, and their interactions with the developing embryo (26, 27, 32, 33). However, none of these suggested models completely replicate normal embryo implantation conditions. Although there are similarities between decellularized tissue and native endometrium, there is limited research on the use of decellularized tissue to establish an *in vitro* implantation model (9). Campo et al. (9) have demonstrated that tissue-specific ECM-derived hydrogels obtained from rabbit endometrial decellularized tissues at different stages could facilitate rabbit morula stage embryos to proliferate and grow for 48 hours. Lü et al. (26) reported successful *in vivo* embryo implantation and development after transplantation of rabbit endometrial decellularized tissue in an induced damaged endometrial tissue model.

Ethical and legal limitations preclude *in vivo* human embryo implantation experiments; therefore, an implantation model that uses a natural endometrial scaffold and surrogate embryo could provide an alternative approach to better understand the implantation process. In the current study, we first evaluated the interaction of mouse blastocysts as a surrogate embryo on a recellularized endometrial scaffold with human endometrial mesenchymal cells (hEMCs). The effect of mouse embryos on the induction of a decidualization reaction in the seeded cells was studied at the morphological and molecular levels.

Materials and Methods

All materials used in this study were obtained from Sigma Aldrich (London, UK) unless otherwise noted.

Study design

In this experimental study, decellularized the endometrial tissue fragments were evaluated for morphology, ultrastructure, and DNA content. Cytotoxicity of the decellularized scaffold (DS) was investigated using the 3-(4, 5-dimethyl thiazolyl-2)-2, 5-diphenyltetrazolium bromide (MTT) assay. hEMCs were mechanically and enzymatically separated from fresh tissues and cultured until the fourth passage, and then characterized them by inverted microscopy and flow cytometry analyses. The generated scaffolds were recellularized by seeding the hEMCs for seven days, and subsequently, the mouse blastocysts were co-cultured on this DS for 24 and 48 hours. Finally, the mouse embryo implantation was evaluated by morphological, ultrastructural, molecular, and hormonal studies and compared with the control group.

Human endometrial tissue collection

The Ethics Committee of the Faculty of Medicine of Tarbiat Modares University, Tehran, Iran (IR.MODARES.REC.1400.209) approved this experimental study. A total of eight fertile women, 25 to 35 years of age, diagnosed with gynaecologic diseases other than endometrial disease provided informed consent for the collection and use of their endometrial tissues. The women did not undergo any exogenous hormone treatment within three months before sample collection. The collected samples were transferred to the laboratory in Dulbecco's Modified Eagle's medium (DMEM) on ice supplemented with 100 IU/ml penicillin, and 100 µg/ml streptomycin for 1-2 hours. The endometrial tissues were cut into ~2-3 cm^2 pieces (total: 70 pieces from eight women). The normality of the tissue was analysed and confirmed by an expert pathologist (n=2 pieces per sample). The other tissue fragments were used for decellularization and endometrial cell isolation and culture.

Decellularization of endometrial tissue

Tissue decellularization was done according to a previous study protocol (21). Briefly, the endometrial tissue samples were subjected to three freeze/thaw cycles at -80°C and 37°C, respectively. Next, the samples were incubated in 1% Triton X-100 at room temperature while placed on a rotator for 15 hours and in 1% sodium dodecyl sulphate (SDS) for 72 hours. Finally, they were washed at room temperature with phosphate buffer saline (PBS) for 48 hours. Some of the samples were assessed for DNA content, morphological staining, and ultrastructural study by scanning electron microscopic (SEM) analysis.

Morphological evaluations

The decellularized and native control tissues (n=5 fragments per group) were fixed with 10% formaldehyde, dehydrated in increasing concentrations of ethanol, and embedded in paraffin. Then, 5 µm-thick tissue sections were prepared, and six series of tissue sections were collected after deparaffinization and hydration for morphological evaluation by haematoxylin and eosin (H&E), Masson's trichrome, Alcian blue, periodic acid schiff (PAS), Van Gibson's and Orcein staining. Morphology of the tissue sections, presence or absence of a nucleus, and content of collagen fibres, glycosaminoglycans (GAGs),

carbohydrates, and elastin fibres were examined by light microscope. A total of three samples per group were used for the ECM study.

DNA content analysis

DNA extraction was performed in DS (n=6) and native tissue (n=3) using a TRIzol® kit (Invitrogen, UK) according to defined protocols. For this purpose, the samples were weighed and treated with TRIzol® reagent, then chloroform was added. The DNA layer was separated and centrifuged at 2000 g for 10 minutes at 4°C, resuspended in NaOH, and centrifuged again at 12 000 g for 10 minutes at 4°C. Finally, the DNA content was measured by UV spectrophotometry (Eppendorf, Germany) at 260 nm optical density and reported as ng/mg wet tissue.

Cell isolation and culture

The endometrial tissue fragments (n=5 patients) were washed in PBS, cut into 1 mm pieces in DMEM/F-12 (Invitrogen, UK) that contained 100 mg/ml penicillin G sodium, 100 mg/ml streptomycin sulphate B, and 10% foetal bovine serum (FBS, Invitrogen, UK). The tissues were then subjected to collagenase type I (300 µg/ ml) and deoxyribonuclease type I (40 µg/ml) for 60-90 minutes. The isolated endometrial stromal cells were cultured to the fourth passage at 37°C in 5% CO_2 (24).

The collected cells were evaluated for mesenchymal (CD90, CD44), hematopoietic (CD45), and endothelial (CD31) markers by flow cytometry analysis.

A total of 1×10^5 endometrial cells were suspended in 50 µl of PBS and incubated with direct isothiocyanate (FITC)-conjugated antibodies (anti-human CD90, CD44, and CD45, 1:50 dilution) and direct phycoerythrin (PE)-conjugated antibodies (anti-human CD31; 1:50 dilution) at 4 °C for 45 minutes. Finally, 200 µl of PBS was added and the cells were examined by FACSCalibur apparatus (Becton Dickinson, USA). These analyses were repeated three times.

3-(4, 5-dimethyl thiazolyl-2)-2, 5-diphenyltetrazolium bromide (MTT) assay

Each DS (n=6) was placed in a 96-well plate that contained 200 µ of DMEM/F12 and 1×10^6 endometrial mesenchymal cells, and cultured for 24 and 72 hours. The DS and media were removed and 100 µL of MTT solution (1 mg/mL of MTT in PBS) was added to each well that contained the remaining cells and they were incubated for 4 hours. Then, the MTT solution was replaced by dimethyl sulfoxide and the cells were allowed to incubate in a dark room for 20 minutes. Optical density was read immediately at 540 nm using a microplate reader (Biochrom, Germany) and compared with cells not exposed to scaffolds under the same condition as described earlier as the control group.

Recellularization of endometrial scaffolds

DS fragments were individually placed in each well of a 24-well plate (n=30 scaffolds) that contained DMEM/F-12 media supplemented with 100 mg/ml penicillin G sodium, 100 mg/ml streptomycin sulphate B, and 10% FBS. Next, we added 1×10^6 hEMCs to each well and the plates were incubated at 37°C in 5% CO_2 for seven days. The medium was changed every two days. At the end of the culture period, the morphology of the recellularized scaffold was studied by H&E and Masson's trichrome, Alcian blue, PAS, Van Gieson's, and Orcein staining. In addition, the ultrastructure of the recellularized scaffolds was assessed by SEM.

Mouse blastocyst collection and labelling

The 6-8-week-old female mice (n=70) and 8-12-week-old male mice (n=10) were obtained from the Naval Medical Research Institute at kept under standard conditions for laboratory animals at Tarbiat Modares University, Tehran, Iran. Each adult female mouse received an intraperitoneal injection of 7.5 IU of pregnant mare serum gonadotropin (Folligan, Intervet, Australia) followed by another intraperitoneal injection of 10 IU of human chorionic gonadotropin (Pregnyl, Netherlands). Then, the female mice were individually mated with fertile males. After 120 hours from the last injection, the blastocysts were flushed from the uterine horns and collected in media until co-culturing.

Blastocyst co-culture with recellularized scaffold

Seven days after recellularization of DS with hEMCs, the mouse blastocysts were placed on top of each scaffold (n=5 embryos per well) in DMEM/F-12 media supplemented with 100 mg/ml penicillin G sodium, 100 mg/ml streptomycin sulphate B, and 10% FBS for 24 and 48 hours at 37°C in 5% CO_2. This group was considered to be the experimental group (n=15 scaffolds). Recellularized scaffold without mouse blastocysts comprised the control group (n=15 samples). The control group was incubated the same conditions as the experimental group (48 hours at 37°C in 5% CO_2). Some of the samples from the experimental and control groups were collected, fixed, and processed as described earlier for morphological analysis by H&E staining (n=3 per group). Other samples were used for SEM, laser confocal scanning microscope (LCSM), and molecular studies. Some of the culture media were collected after 24 and 48 hours for hormonal analysis.

Scanning electron microscopic analysis

We evaluated the ultrastructure of the native, decellularized tissue, and recellularized scaffold co-cultured with and without embryo (n=3 for each group at each time). These samples were collected and fixed in 2.5% glutaraldehyde and dehydrated in ascending concentrations of ethanol (50, 60, 70, 80, 90, 96 and 100%, respectively). The dehydration process was

completed with a mixture of hexamethyldisilazane and ethanol at ratios of 1:2 (20 minutes) and 2:1 (20 minutes), respectively, and the samples were incubated overnight in 100% hexamethyldisilazane. The samples were coated with a thin layer of gold and observed under SEM (VEGA/TESCAN-XMU, Czech Republic).

Laser confocal scanning microscope study

We used an LCSM (Zeiss LSM800, Japan) to study the ability of the mouse blastocysts to penetrate the DS. In order to identify and track the blastocysts within the scaffolds, we incubated the collected blastocysts with Hoechst dye for 20 minutes and then washed them with DMEM for 20 minutes. The labelled mouse blastocysts were co-cultured with a DS as previously described and detected with the blue channel (400-550 nm wavelength) after 48 hours.

Gene expression analysis

We used the TRIzol® kit (Invitrogen, UK) to extract total RNA from the recellularized scaffold on day 7. and that was co-cultured with or without mouse embryos on day 9 of the culture period (n=3 samples per group). Endometrial tissue was used as the positive control and hEMCs cultured in the absence of any scaffold comprised the negative control group.

cDNA was synthesized according to a cDNA synthesis kit (Thermo Fisher Scientific, EU) after extraction of the total RNA. The primers were designed with AllelID 7.8 software for the target genes *ZO-1, SPP1, COL4-A1, MMP2,* and *PRL* and for the housekeeping gene, *β-actin*. Table 1 lists the details of the primers. SYBR Green Supermix (Bio-Rad) was used in a real-time RT-polymerase chain reaction (PCR) reaction; after each PCR run, the reaction accuracy was checked by melting and amplification curves. Relative expressions of the studied genes to the reference gene were calculated with the $2^{-(\Delta\Delta CT)}$ formula and compared between the groups. The real-time RT-PCR product was confirmed by gel electrophoresis analysis.

Hormonal assays

We evaluated the function of these surrogate embryos and decidual cells by analysing Beta human chorionic gonadotropin (β-hCG) and prolactin hormone levels in the collected media at 24 and 48 hours after the mouse embryos were co-cultured with recellularized endometrial tissue and in their controls (n=3 for each group). β-hCG and prolactin levels were measured by electrochemiluminescence with commercial kits (Roche). The experiments were done in triplicate.

Statistical analysis

All experiments were conducted at least in triplicate and statistical analysis was performed using SPSS software (V24, SPSS, Inc., Chicago, IL, USA). The Shapiro-Wilk normality test was carried out to confirm the normality distribution of the data. One-way analysis of variance followed by post hoc Tukey's Honest Significant Difference test was done for pairwise comparison of the means of the DNA content. The Independent Sample Student t test was used for pairwise comparison of the results of the MTT test, real-time RT-PCR, and hormone levels. $P<0.05$ indicated statistical significance.

Table 1: Primers used for the real-time reverse transcriptase polymerase chain reaction (RT-PCR) reaction

Target gene	Primer pair sequences	Accession number	Fragment size (bp)	Tm (°C)
ZO-1	F: GAGGATGAAGATGAAGATGGT	NM_003257.5	183	59-36
	R: TGGAAGGATGCTGTTGTC			57-99
SPP1	F: TCTGATGAATCTGATGAACTG	NM_000582.3	194	57-56
	R: GTGATGTCCTCGTCTGTA			56-42
COL4A1	F: AGGAGCGAGATGTTCAAG	NM_001845.6	148	57-45
	R: AAGAAGAAGAAGTAGCACCAT			57-13
MMP2	F: GGAGATACAATGAGGTGAAGA	NM_004530.6	96	63-14
	R: CGACGGCATCCAGGTTAT			61-45
PRL	F: CCTTCGAGACCTGTTTGACCG	NM_000948.6	153	63
	R: GTGGCAAGGGAAGAAGTGTGG			63
β-actin	F: CAAGATCATTGCTCCTCCTG	NM_001101.3	90	60.5
	R: ATCCACATCTGCTGGAAGG			60.5

Results

Morphological observations

Figure 1A shows the gross morphology of the native and decellularized endometrial tissues. In this Figure, the DS sample is white compared with the native tissue.

Representative light microscopic micrographs of the H&E stained tissues are shown in Figure 1B and C. The gland, epithelial, and fibroblast-like flattened stromal cells in the native tissue had normal morphology. There was no morphological evidence of cells and nuclei in the DS tissue section.

DNA content analysis

The amount of DNA in the control group was 935.151 ± 18.104 ng/mg of wet tissue compared to 94.303 ± 6.038 ng/mg in the decellularized group (Fig.1D). The DNA content significantly decreased by 89.92% in the decellularized group compared to the control group ($P<0.05$).

Light microscopic observation of the extracellular matrix

Figure 2A-J shows light microscopic observations of the ECM components in the stained native and DS.

Masson's trichrome staining showed that the nuclei were dark brown to black; the smooth muscle cell stained red and the collagen fibres were blue. A similar pattern of collagen bundles was observed in the native (Fig.2A) and DS (Fig.2F) groups. The vascular structure was well preserved in decellularized tissue (black arrow).

Alcian blue staining was performed to investigate GAG content. We observed purple nuclei and green-stained GAG. Distribution of the GAGs in the stroma and blood vessels were similar in DS and native tissues. Figure 2B and G show representative micrographs of these two groups.

PAS-positive reactions were observed in the ECM of the glandular and surface epithelium of the control group (Fig.2C) and within the stroma of the control and decellularized endometrium (Fig.2H).

Van Gieson (Fig.2D, I) and Orcein (Fig.2E, J) staining results showed a similar pattern of collagen bundles and elastin fibers in both studied groups.

Light microscopy observations of the recellularized scaffolds stained with Masson's trichrome, Alcian blue, PAS, Van Gibson's, and Orcein staining are presented in Figure 2K-O.

This figure also shows that after one week of *in vitro* culture, the cells appear scattered within different parts of the tissue, and the stromal structure and components have similar morphology to the native samples.

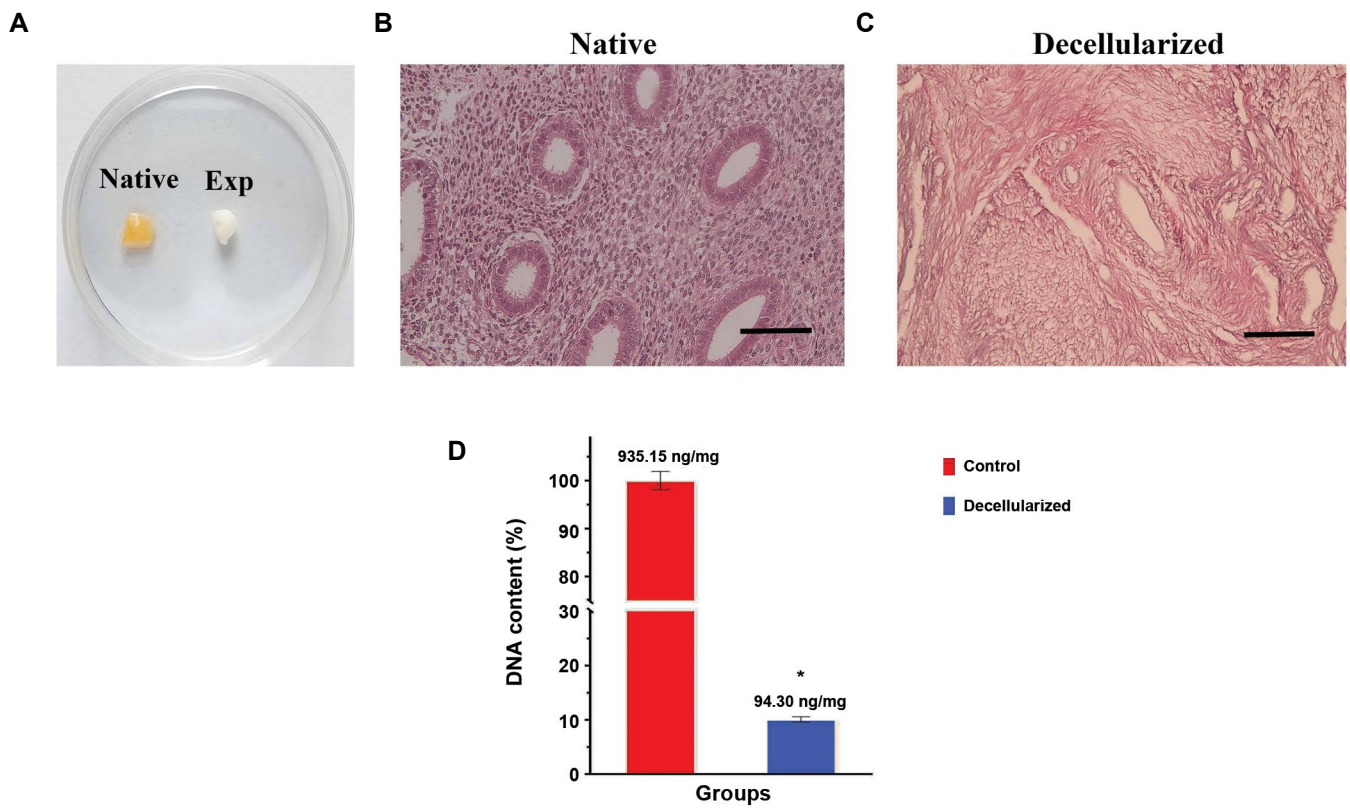

Fig.1: The macroscopic and microscopic observations of decellularized and control tissues. **A.** Gross morphology of human native and decellularized endometrial tissues. **B.** Light microscopic observation of human endometrial tissue after hematoxylin and eosin (H&E) staining shows the normal structure of endometrial tissue with several glands (scale bar: 100 µm) and **C.** Decellularized tissue with no stained nucleus (scale bar: 100 µm). **D.** A comparison of the amount of DNA in both groups. This experiment was conducted in triplicate. Data are shown as mean ± SD. *; Significant difference between groups ($P<0.05$).

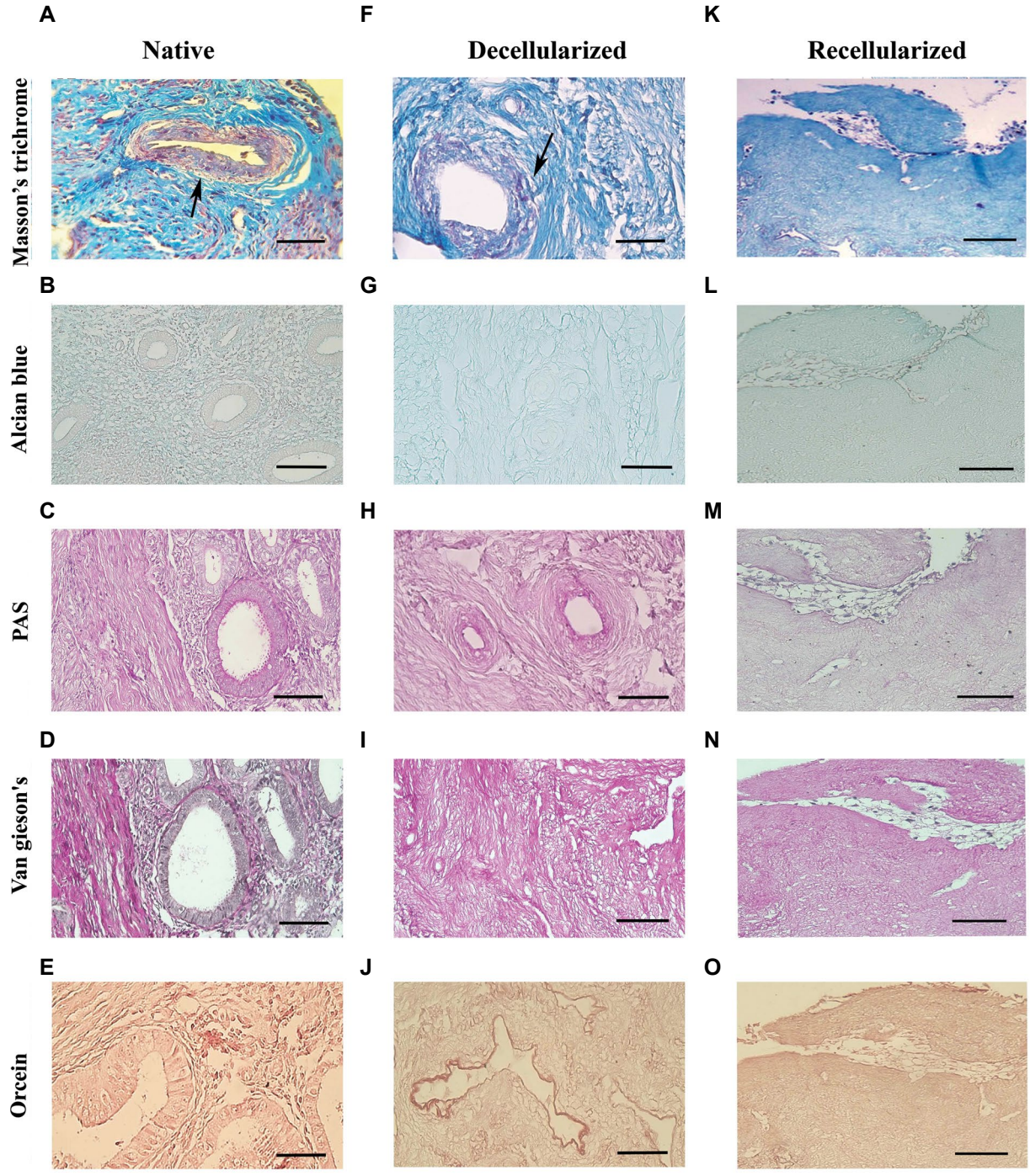

Fig.2: Light microscopic observations of the native and decellularized tissue after morphologic staining for different components of the ECM. **A-E.** Representative micrographs of control or native endometrium (first column) and **F-J.** decellularized tissues (second column) stained by Masson's trichrome for collagen; Alcian blue for Glycosaminoglycans; Periodic acid Schiff (PAS) for carbohydrates; Van Gieson's for collagen; and Orcein staining for elastin are shown in the first to fifth rows, respectively. **K-O**. The third column shows the morphology of the recellularized tissue using endometrial mesenchymal cells after one week of cultivation (scale bars: A, E, F, J, K-O; 100 µm and B-D, G-I; 120 µm).

Characteristics of human endometrial mesenchymal cells

The endometrial stromal cells adhered to the bottom of the culture dish and took on a spindle-shaped appearance. Gradually cell proliferation began, and after the fourth passage, the cultured cells had an almost homogeneous spindle-shaped appearance. These endometrial stromal cells had normal mesenchymal cell surfaces markers, CD90 (98.60 ± 1.64%) and CD44 (99.8 ± 1.03%), and they were negative for CD45 (0.96 ± 0.02%) and CD31 (0.38 ± 0.19%), hematopoietic and endothelial markers (Fig.3A-F).

Cytotoxicity assessment

We performed the MTT assay on endometrial cells

cultured with DS. The observed optical density in the control group was 0.284 ± 0.03 after 24 hours and 0.406 ± 0.017 after 72 hours. Optical densities in the DS group were 0.294 ± 0.031 (24 hours) and 0.415 ± 0.014 (72 hours). There was no significant difference in optical density between these two groups during the culture period; however, there was a statistical increase in cell proliferation observed in both groups after 72 hours of cultivation (P<0.05, Fig.3G).

Light microscopic observation of the recellularized scaffold with human endometrial mesenchymal cells

Figure 4A and B show the morphology of H&E stained hEMCs-seeded cells on the DS after one week of *in vitro* culture at low and high-power magnifications. Figure 4C and D show the morphology of recellularized DS after nine days. The hEMCs attached to the surface and penetrated and infiltrated within different parts of the scaffolds.

Light microscopic observation of co-cultured embryos on the recellularized scaffold

Figure 4E-H shows the light microscopic images of mouse blastocysts co-cultured on this recellularized scaffold after 24 and 48 hours. The embryo was attached to the surface of the scaffold after 24 hours (Fig.4E, F, red arrow) and was surrounded by several seeded cells. The mouse embryos penetrated into the recellularized endometrial tissue after 48 hours (Fig.4G, H) and its yolk and amniotic sacs could be seen. We observed seeded mesenchymal cells around the embryo (black arrow). Some of the seeded cells formed multi-layered organoid-like structures (Fig.4I).

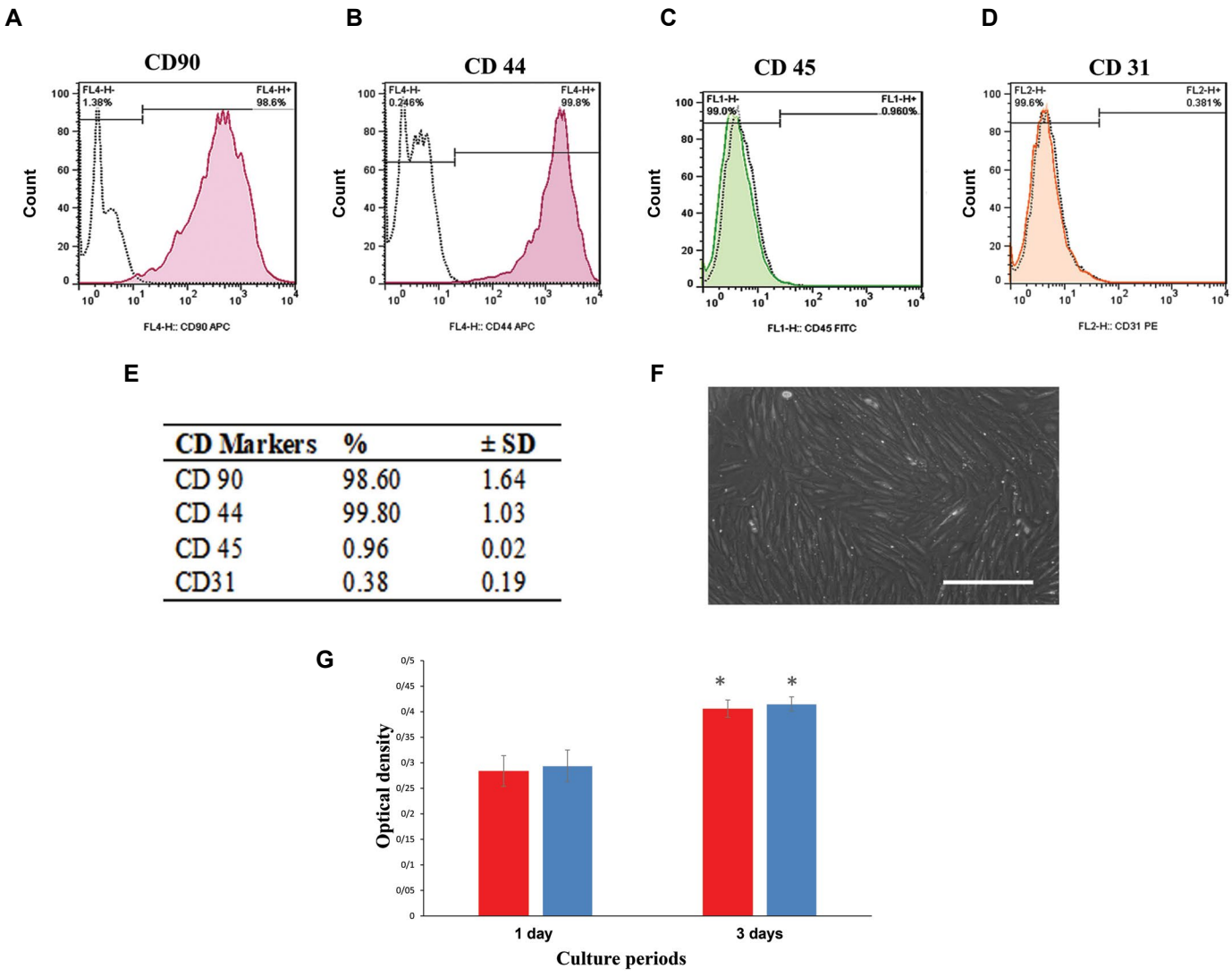

CD Markers	%	± SD
CD 90	98.60	1.64
CD 44	99.80	1.03
CD 45	0.96	0.02
CD31	0.38	0.19

Fig.3: Flow cytometry analysis of endometrial mesenchymal cells. **A.** CD90, **B.** CD44, **C.** CD45, and **D.** CD31 markers. **E.** A summary of their percentages. **F.** Inverted microscopic observation of passage-4 cultured human endometrial cells (scale bar: 50 µm). **G.** Results of the 3-(4, 5-dimethyl thiazolyl-2)-2, 5-diphenyltetrazolium bromide (MTT) assay of the created scaffold seeded by endometrial cells after 24 and 72 hours of cultivation are shown. *; Significant difference with the respected group at 24 hours of culture (P<0.05).

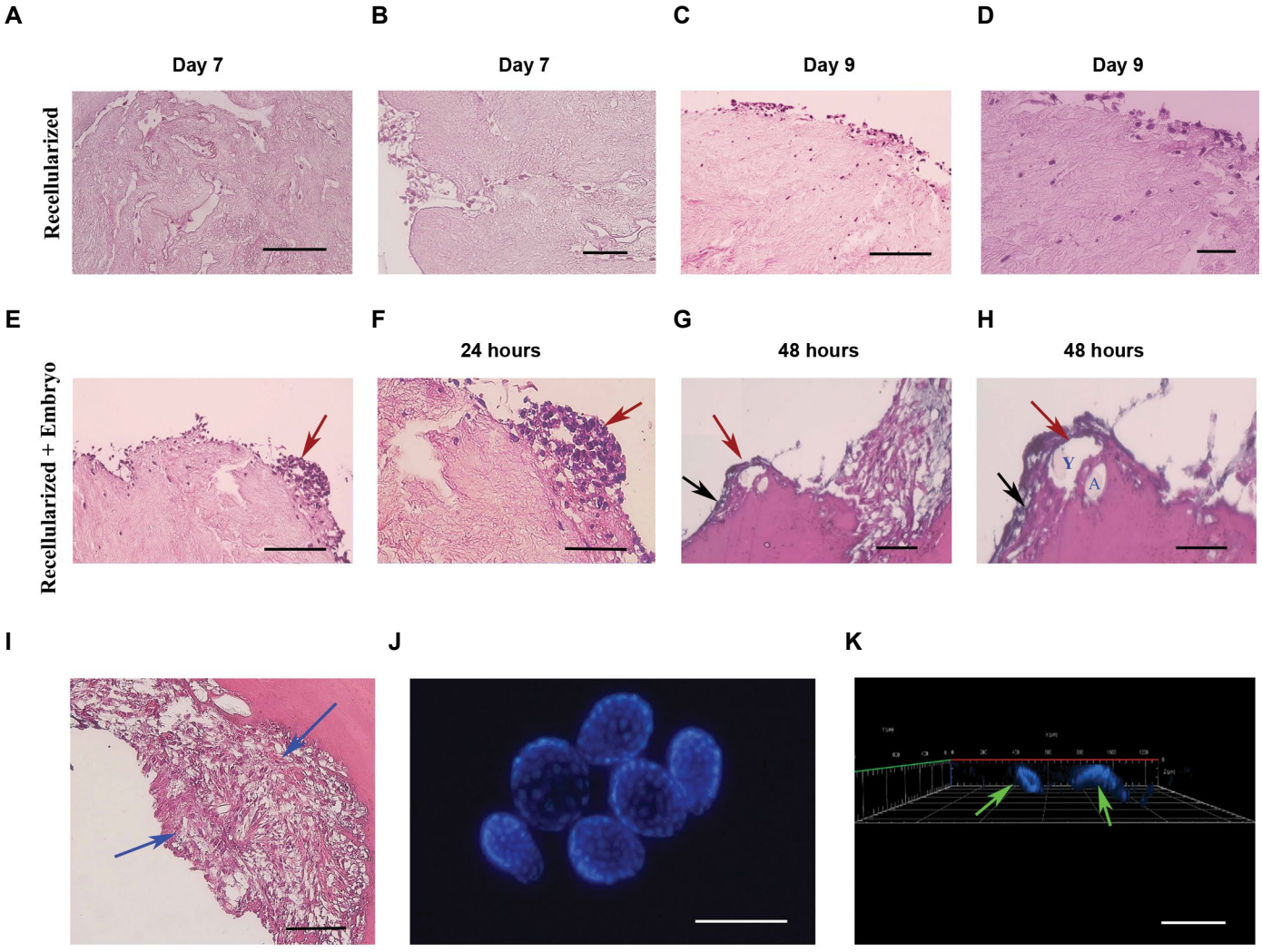

Fig.4: Photomicrographs of recellularized endometrial scaffolds stained with haematoxylin and eosin (H&E). **A-D.** Low and higher magnifications on days 7 and 9 of the cultivation period show that the cells have scattered into the different parts of the scaffold. **E-H.** Attachment of the mouse embryo onto the recellularized scaffold after 24 and 48 hours (red arrow). **G, H.** Penetration by the embryo into the scaffold after 48 hours. Its yolk sac (Y) and amniotic sac (A) can be seen, and there are several endometrial cells around the embryo (black arrow). **I.** A multilayered organoid-like structure is seen in the recellularized group in the presence of the embryo (blue arrow). **J.** Representative figures of mouse embryos labelled with Hoechst 34580, and **K.** Their penetration within the scaffold as captured by confocal laser scanning microscopy (scale bars: A-E, G, J; 100 µm, F, H; 60 µm, I; 50 µm, K; 120 µm)

Laser confocal scanning microscope observation of co-cultured embryos on the recellularized scaffolds

In order to trace the mouse blastocysts, we stained them with Hoechst 34580 dye before cultivation (Fig.4J). The 3D figures captured by LCSM imaging (Fig.4K) show confirmed the presence of the Hoechst-labelled embryos within the recellularized scaffold. The visualized blue-labelled embryos had implanted to a depth of 200 µm within the scaffold.

Scanning electron microscopic observation of co-cultured embryo on the recellularized scaffold

The SEM micrographs show the presence of cells in the native endometrial tissue (Fig.5A, white arrows), while there was no evidence of cells in the decellularized endometrium. Bundles of collagen fibre within the stromal tissue and around the vascular structure are well preserved in the DS (Fig.5B, white arrowhead). SEM images of the recellularized scaffold after one week of cultivation show the presence of seeded cells on the surface and within the stroma of the DS. The cells had spindle shape and polyhedral morphology (Fig.5C, D, yellow arrow).

The embryos attached to the recellularized endometrial scaffold after 24 hours of co-culture (Fig.5E, F, red arrow). We observed vertical growth of the embryos. However, the cylindrical view of the embryo was observed with the formation of a well-defined pore surrounded by the epiblast cells (Fig.5G, H). A number of prominent projections on the surface of the seeded mesenchymal cells were located adjacent to the attached embryo (red arrowhead).

Molecular analysis of co-cultured embryo on the recellularized scaffold

We evaluated the expressions of *ZO-1, SPP1, COL4-A1, MMP2,* and *PRL* to *β-actin* in the recellularized scaffolds co-cultured with and without mouse embryos on culture day 9 to the cell-seeded scaffold on day 7 of the culture (control group). Figure 6A-E shows the relative expressions of *ZO-1* and *COL4A1* as epithelial-related genes to *β-actin*. Relative expression of *ZO-1* was 0.49 ± 0.02 and 0.67 ± 0.16 for *COL4A1* in the recellularized group in the presence of embryo; these ratios were 056 ± 0.02 (*ZO-1*) and 083 ± 0.02 (*COL4A1*) in the group without the embryo. *ZO-1* had significantly lower expression in the recellularized group on day 7 as the control group (0.57 ± 0.03) in comparison with the two recellularized groups in the presence or absence of embryo on day 9 of the culture period (P<0.05). There was no significant difference between the studied groups on day 9 and day 7 regarding *COL4A1* expression.

The relative expressions of the stromal-specific and decidualization-related genes to *β-actin* were 0.51 ± 0.24 (*SSP1*), 0.56 ± 0.02 (*MMP2*), and 0.26 ± 0.07 (*PRL*) in the recellularized group on day 9 in the presence of embryo; these ratios were 0.62 ± 0.17 (*SSP1*), 0.75 ± 0.15 (*MMP2*), and 0.40 ± 0.03 (*PRL*) in the group without the embryo. There was a significant increase in expression levels in the recellularized group co-cultured with the embryos in comparison with the recellularized group in the absence of embryo and the control group on day 7 of the culture period (P<0.05). There was significantly lower *MMP2* and *PRL* expression in the recellularized group on day 7 when compared with both studied groups on day 9 (P<0.05).

Figure 5 shows that all target genes were expressed on normal endometrium [positive control (PC)] and were not expressed in the cells cultured in the absence of any scaffold [negative control (NC)].

Hormonal concentrations

β-hCG levels significantly increased in the recellularized group after 48 hours of co-culture with the embryo compared with day one in this group. Moreover, it is higher than the control group that cultured without an embryo (Fig.6F, G, P<0.05).

Prolactin levels statistically increased in the experimental group in the presence of embryo during the culture period and in comparison with the control group (Fig.5F, G, P<0.05).

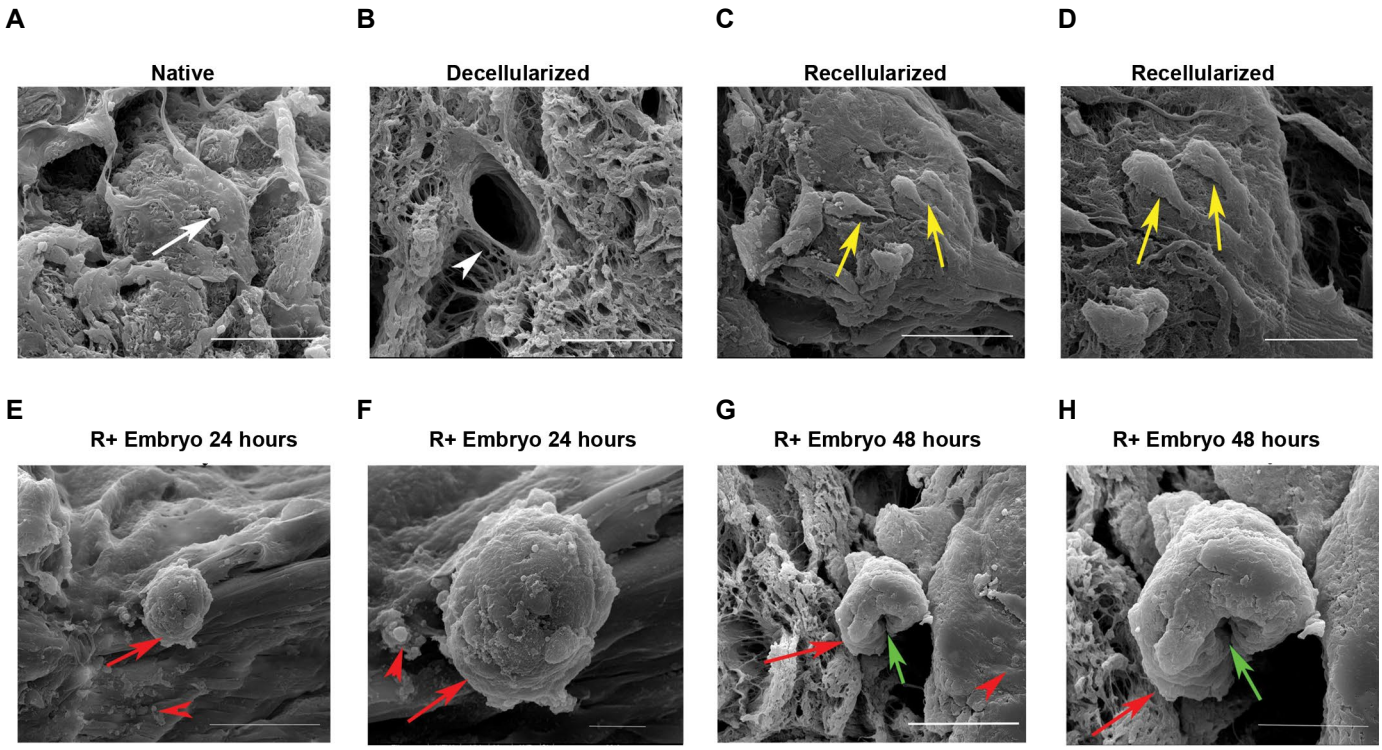

Fig.5: SEM micrographs of de- and recellularized scaffolds (R). **A.** The white arrow shows the presence of cells within native tissue. **B.** There is no evidence of cells in the decellularized endometrium and the normal structure of blood vessels in this sample is demonstrated. **C, D.** The yellow arrows show the attachment of several hEMCs to the scaffold after one week of cultivation. **E-H.** Attachment of the mouse embryos on the recellularized scaffold after 24 and 48 hours of co-culture (red arrow). **E-G.** Projections are seen on the surface of the seeded mesenchymal cells (red arrowhead). **G, H.** The lumen of the pro-amniotic cavity surrounded by epiblast cells is prominent after 48 hours of culture (green arrows) (Scale bars: A, D, F; 20 µm, B, C, H; 50 µm, E, G; 100 µm). SEM; Scanning electron microscopic, hEMCs; Human endometrial mesenchymal cells, and R; Recellularized.

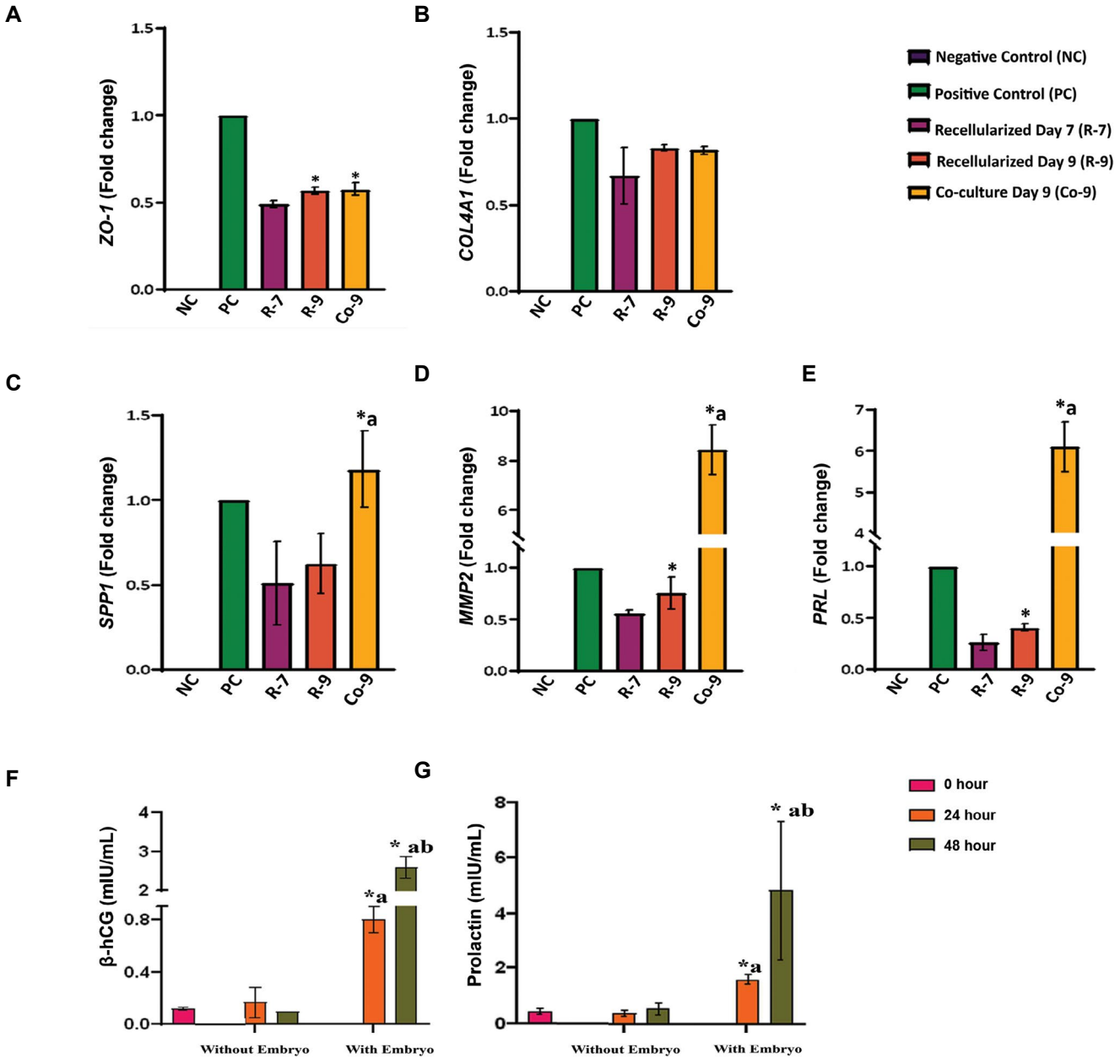

Fig.6: Relative expressions of target genes to *β-actin* in the studied groups. All target genes **A.** *ZO-1,* **B.** *SPP1,* **C.** *COL4-A1,* **D.** *MMP2,* and **E.** *PRL* are expressed in the human endometrium, as the positive control (PC). There was no expression related to the studied genes in the endometrial mesenchymal cells that were cultured without any scaffold, as the negative control (NC). Higher expression ratios of the target genes are seen in the recellularized group co-cultured with the embryos (Co-9). A comparison of the levels of **F.** β-hCG and **G.** prolactin in the studied groups. *; Significant difference with day 0 (P<0.05). All experiments were conducted in triplicate. Data are shown as mean ± SD. *; Significant difference with the recellularized group on day 7 (R-7) of the culture period (P<0.05), a; Significant difference with the recellularized group in the absence of an embryo (P<0.05), and b; Significant difference with the recellularized group in the presence of an embryo at 24 hours of the culture period (P<0.05).

Discussion

This study assessed an implantation model of decellularized endometrial tissue that used hEMCs and mouse blastocysts. Initially, we evaluated the characteristics of the endometrial DS by comparing it with a native sample. The efficacy of the decellularization procedure depends on the thickness, density, and cellularity of the tissue in addition to the type of decellularization technique. Similar to our previous work, we observed that the applied protocol effectively removed a high amount of DNA and cellular materials, and adequately preserved the ECM components. Our findings were confirmed by morphological staining. The preservation of essential molecules of the stroma - collagen, elastic fibers, carbohydrate or PAS-positive materials, and GAGs provides a suitable architecture for cell attachment, penetration, and homing, and can facilitate cell proliferation and differentiation (34). Collagen is a major protein in the ECM that, along with other structural proteins, plays a critical role in tissue regeneration because it forms the basic molecule for cell attachment and homing. In addition, the preservation of the integrity of blood vessels provides an alternative path for the migration and distribution of seeded cells. ECM proteins have been shown to play a role as carriers for the release of growth factors

critical for cell function and behavior (9). These findings supported the results of other investigations (17-19, 23); although, some studies used ribonuclease as an enzymatic digestion treatment (17-19). An advantage of our protocol is the decellularization of tissue without any enzymatic treatment; this additional procedure appeared to affect both the stability and integrity of the tissue. The biocompatibility test of this created scaffold showed that it did not have any cytotoxic effect, and its physical and biological characteristics could adequately support cell adhesion and proliferation.

Endometrial mesenchymal cells are responsible for the cyclical repair of the endometrium during the menstrual cycle. In this study, we used these cells to recellularize the scaffold. Prior to cell seeding, we characterized the passage-4 cultured cells. The purification of these isolated and cultured cells was high and 98.6% CD90, and 99.8% expressed CD44, as mesenchymal cell markers. One week after cell seeding, these cells attached and penetrated different thicknesses of the created scaffold. Light microscopy and SEM micrographs indicated a close interaction between the seeded cells and the ECM. The ECM proteins of the endometrial scaffold or natural niche are proposed to facilitate attachment and homing of these cells, and have inductive effects on cell proliferation and differentiation, which is similar to normal endometrial conditions (35).

For the first time, the interaction between mouse blastocysts and the recellularized endometrial tissue was evaluated. Micrographs obtained after 24 hours of embryos co-cultured with these created scaffolds revealed that the embryonic cells attached to the surface of the scaffold. The embryo attachment site had more aggregation of hEMCs-seeded cells around the embryonic pole. The seeded cells appeared to have more potential to interact with each other and with embryonic cells to facilitate the implantation process. Interactions between the embryonic cells and endometrial cells are critical for implantation of an embryo. This bidirectional interaction is mediated by adhesion molecules that include laminin, collagen, and fibronectin and their transmembrane receptors (36). Adequate preservation of these proteins during the decellularization procedure seems to support the attachment and invasion of an embryo within the DS, similar to the *in vivo* condition. H&E-stained tissue results revealed that after 48 hours of co-culture, the mouse embryo could penetrate within the scaffold, and develop and progress to the egg cylinder stage with prominent yolk and amniotic sacs. The implantation process involves three main steps: apposition and establishment of cross-talk between the embryo and endometrial cells, trophoblast attachment to the epithelial layer, and invasion of embryonic cells into the underlying stroma. This invasion is facilitated by the release of enzymes from trophoblastic cells and by the presence of suitable porosity in the scaffold that supports embryonic movement and invasion, which was confirmed by SEM images. From another point of view, it is proposed that the endometrial seeded cells produce different growth factors and secretory materials that facilitate and improve embryo implantation. However, it seems that the bidirectional interaction of embryo and seeded cells could influence these cells to differentiate into decidual cells. In comparison with other types of implantation models, the cell-cell and cell-ECM interaction and contact were better established, and trophoblast invasion was facilitated in the applied model in the present study. This finding was confirmed by our molecular studies. At the mRNA level, we analyzed the expressions of target genes in hEMCs seeded on the created scaffold co-cultured in the presence or absence of mouse embryos. Epithelial-related and decidual cell-related genes were evaluated (2, 24, 25). Our results revealed that *ZO-1* and *COL4A1* expressed in both recellularized groups, while any gene expression was seen in cells cultured alone and without scaffolds. This observation confirmed the inductive effect of the endometrial scaffold to differentiate hEMCs into epithelial-like cells. Expression of the collagen IV gene, as the main marker of the basement membrane, demonstrated the potential formation of polarized epithelial cells by hEMCs. This finding supported results from other investigations (37). The expression of ZO-1, as a tight junction protein, shows the ability of these seeded cells to establish an intercellular tight junction and the formation of epithelial cells (38). The presence of an embryo in the recellularized group had the inductive effect to initiate the decidualization process in seeded cells. *SPP1, MMP2,* and *PRL* expressions increased during the culture period.

Osteopontin and matrix metalloproteinase (MMP) proteases are secreted by endometrial epithelial and stromal cells; they play critical roles in cell-to-cell adhesion, endometrial cell proliferation, and migration during embryo implantation and endometrial tissue remodelling (39).

In a similar manner, there was an increase in prolactin release in the collected media in the recellularized scaffolds that were co-cultured with mouse embryos. Prolactin synthesis increases in human endometrium from the late luteal phase of the menstrual cycle and throughout pregnancy by decidual cells. Prolactin secretion regulates the differentiation and formation of endometrial glands. Its function is concentration dependent. Low concentrations of prolactin stimulate endometrial cell growth and inhibit it at higher concentrations (40).

β-hCG production is a good indication of the vital and well-developed status of an embryo. Thus, we analyzed β-hCG levels in the media collected after co-culture of mouse blastocysts with the recellularized endometrial scaffold. Our results demonstrated increased secretion of this hormone during the co-culture period. However, additional assessments to determine the survival rate of embryos during the culture period could be effective. The selection of suitable cultural media is another challenging area in this system. Adjustments of the culture media for both embryonic and somatic cells are very important and could affect the results.

Because human blastocysts are not available in sufficient numbers, we suggest that the present model that uses human endometrial cells, decellularized endometrium, and mouse embryos could provide a good alternative implantation model to identify the molecular mechanisms involved in embryo implantation. The establishment of this model requires additional studies.

Conclusion

The co-culture of hEMCs and mouse embryos into a decellularized endometrial scaffold provides an alternative model to study embryo implantation and the earlier stage of embryo development.

Acknowledgments

This research project was extracted from a Ph.D. thesis supported by Tarbiat Modares University, Tehran, Iran. The authors declare that there were no commercial or financial relationships that could be construed as potential conflicts of interest.

Authors' Contributions

M.S.; Supervised the study, provided technical assistance, and prepared the manuscript. E.S.; Performed the experiments, conducted data analysis, and contributed to writing this manuscript. M.R.V.; Was the scientific research assistant and co-supervised this study. All authors read and approved the final manuscript.

References

1. Li X, Kodithuwakku SP, Chan RWS, Yeung WSB, Yao Y, Ng EHY, et al. Three-dimensional culture models of human endometrium for studying trophoblast-endometrium interaction during implantation. Reprod Biol Endocrinol. 2022;20: 1-19.
2. Fayazi M, Salehnia M, Ziaei S. In-vitro construction of endometrial-like epithelium using CD146(+) mesenchymal cells derived from human endometrium. Reprod Biomed Online. 2017; 35(3): 241-252.
3. Schutte SC, James CO, Sidell N, Taylor RN. Tissue-engineered endometrial model for the study of cell-cell interactions. Reprod Sci. 2015; 22(3): 308-315.
4. Yokomizo R, Fujiki Y, Kishigami H, Kishi H, Kiyono T, Nakayama S, et al. Endometrial regeneration with endometrial epithelium: homologous orchestration with endometrial stroma as a feeder. Stem Cell Res Ther. 2021; 12(1): 1-13.
5. Fitzgerald HC, Schust DJ, Spencer TE. In vitro models of the human endometrium: evolution and application for women's health. Biol Reprod. 2021; 104(2): 282-293.
6. Yoshimasa Y, Maruyama T. Bioengineering of the uterus. Reprod Sci. 2021; 28(6): 1596-1611.
7. Rawlings TM, Makwana K, Tryfonos M, Lucas ES. Organoids to model the endometrium: implantation and beyond. Reprod Fertil. 2021; 2(3): R85-R101.
8. Cramer MC, Badylak SF. Extracellular matrix-based biomaterials and their influence upon cell behavior. Ann Biomed Eng. 2020; 48(7): 2132-2153.
9. Campo H, García-Domínguez X, López-Martínez S, Faus A, Vicente Antón JS, Marco-Jiménez F, et al. Tissue-specific decellularized endometrial substratum mimicking different physiological conditions influences in vitro embryo development in a rabbit model. Acta Biomater. 2019; 89: 126-138.
10. Francés-Herrero E, Juárez-Barber E, Campo H, López-Martínez S, de Miguel-Gómez L, Faus A, et al. Improved models of human endometrial organoids based on hydrogels from decellularized endometrium. J Pers Med. 2021; 11(6): 504.
11. López-Martínez S, Campo H, de Miguel-Gómez L, Faus A, Navarro AT, Díaz A, et al. A natural xenogeneic endometrial extracellular matrix hydrogel toward improving current human in vitro models and future in vivo applications. Front Bioeng Biotechnol. 2021; 9: 639688.
12. Keane TJ, Swinehart IT, Badylak SF. Methods of tissue decellularization used for preparation of biologic scaffolds and in vivo relevance. Methods. 2015; 84: 25-34.
13. Mendibil U, Ruiz-Hernandez R, Retegi-Carrion S, Garcia-Urquia N, Olalde-Graells B, Abarrategi A. Tissue-specific decellularization methods: rationale and strategies to achieve regenerative compounds. Int J Mol Sci. 2020; 21(15): 5447.
14. Santoso EG, Yoshida K, Hirota Y, Aizawa M, Yoshino O, Kishida A, et al. Application of detergents or high hydrostatic pressure as decellularization processes in uterine tissues and their subsequent effects on in vivo uterine regeneration in murine models. PLoS One. 2014; 9(7): e103201.
15. Miyazaki K, Maruyama T. Partial regeneration and reconstruction of the rat uterus through recellularization of a decellularized uterine matrix. Biomaterials. 2014; 35(31): 8791-8800.
16. Hellström M, Bandstein S, Brännström M. Uterine tissue engineering and the future of uterus transplantation. Ann Biomed Eng. 2017; 45(7): 1718-1730.
17. Hiraoka T, Hirota Y, Saito-Fujita T, Matsuo M, Egashira M, Matsumoto L, et al. STAT3 accelerates uterine epithelial regeneration in a mouse model of decellularized uterine matrix transplantation. JCI Insight. 2016; 1(8): e87591.
18. Olalekan SA, Burdette JE, Getsios S, Woodruff TK, Kim JJ. Development of a novel human recellularized endometrium that responds to a 28-day hormone treatment. Biol Reprod. 2017; 96(5): 971-981.
19. Xiao S, Coppeta JR, Rogers HB, Isenberg BC, Zhu J, Olalekan SA, et al. A microfluidic culture model of the human reproductive tract and 28-day menstrual cycle. Nat Commun. 2017; 8: 14584.
20. Jakus AE, Laronda MM, Rashedi AS, Robinson CM, Lee C, Jordan SW, et al. "Tissue Papers" from Organ-Specific Decellularized Extracellular Matrices. Adv Funct Mater. 2017; 27(3): 1700992.
21. Sargazi Z, Zavareh S, Jafarabadi M, Salehnia M. An efficient protocol for decellularization of the human endometrial fragments for clinical usage. Prog Biomater. 2021; 10(2): 119-130.
22. Charoensombut N, Kawabata K, Kim J, Chang M, Kimura T, Kishida A, et al. Internal radial perfusion bioreactor promotes decellularization and recellularization of rat uterine tissue. J Biosci Bioeng. 2022; 133(1): 83-88.
23. Campo H, Cervelló I, Pellicer A. Bioengineering strategies of the uterus towards improving current investigative models and female reproductive health. Facts Views Vis Obgyn. 2019; 11(1): 87-99.
24. Rahimipour M, Jafarabadi M, Salehnia M. In vitro implantation model using human endometrial SUSD2+ mesenchymal stem cells and myometrial smooth muscle cells. Cell J. 2021; 23(2): 154-163.
25. Rahimipour M, Salehnia M, Jafarabadi M. Morphological, ultrastructural, and molecular aspects of in vitro mouse embryo implantation on human endometrial mesenchymal stromal cells in the presence of steroid hormones as an implantation model. Cell J. 2018; 20(3): 369-376.
26. Lü SH, Wang HB, Liu H, Wang HP, Lin QX, Li DX, et al. Reconstruction of engineered uterine tissues containing smooth muscle layer in collagen/matrigel scaffold in vitro. Tissue Eng Part A. 2009; 15(7): 1611-1618.
27. Wang HB, Lü SH, Lin QX, Feng LX, Li DX, Duan CM, et al. Reconstruction of endometrium in vitro via rabbit uterine endometrial cells expanded by sex steroid. Fertil Steril. 2010; 93(7): 2385-2395.
28. Glenister TW. Observations on the behaviour in organ culture of rabbit trophoblast from implanting blastocysts and early placentae. J Anat. 1961; 95(Pt 4): 474-484.
29. Carter AM. Animal models of human pregnancy and placentation: alternatives to the mouse. Reproduction. 2020; 160(6): R129-R143.
30. Ruane PT, Berneau SC, Koeck R, Watts J, Kimber SJ, Brison DR, et al. Apposition to endometrial epithelial cells activates mouse blastocysts for implantation. Mole Hum Reprod. 2017; 23(9): 617-627.
31. Ruane PT, Garner T, Parsons L, Babbington PA, Wangsaputra I, Kimber SJ, et al. Trophectoderm differentiation to invasive syncytiotrophoblast is promoted by endometrial epithelial cells during human embryo implantation. Hum Reprod. 2022; 37(4): 777-792.
32. Bentin-Ley U, Horn T, Sjögren A, Sorensen S, Falck Larsen J, Hamberger L. Ultrastructure of human blastocyst-endometrial interactions in vitro. J Reprod Fertil. 2000; 120(2): 337-350.
33. Chen Y, Fei W, Zhao Y, Wang F, Zheng X, Luan X, et al. Sustained delivery of 17β-estradiol by human amniotic extracellular matrix (HAECM) scaffold integrated with PLGA microspheres for endometrium regeneration. Drug Deliv. 2020; 27(1): 1165-1175.
34. Halper J, Kjaer M. Basic components of connective tissues and extracellular matrix: elastin, fibrillin, fibulins, fibrinogen, fibronectin, laminin, tenascins and thrombospondins. Adv Exp Med Biol. 2014; 802: 31-47.
35. Fuchs E, Blau HM. Tissue stem cells: architects of their niches. Cell Stem Cell. 2020; 27(4): 532-556.
36. Massimiani M, Lacconi V, La Civita F, Ticconi C, Rago R, Campagnolo L. Molecular signaling regulating endometrium-blastocyst crosstalk. Int J Mol Sci. 2019; 21(1): 23.
37. Gatseva A, SinY, Brezzo G, Agtmael TV. Basement membrane collagens and disease mechanisms. Essays Biochem. 2019; 63(3): 297-312.
38. Kuo WT, Odenwald MA , Turner JR, Zuo L. Tight junction proteins occludin and ZO-1 as regulators of epithelial proliferation and survival. Ann N Y Acad Sci. 2022; 1514(1): 21-33.
39. Barbe AM, Berbets AM, Davydenko IS, Koval HD, Yuzko VO, Yuzko OM. Expression and significance of matrix metalloproteinase-2 and matrix metalloproteinas-9 in endometriosis. J Med Life. 2020; 13(3): 314-320.
40. Auriemma RS, Del Vecchio G, Scairati R, Pirchio R, Liccardi A, Verde N, et al. The interplay between prolactin and reproductive system: focus on uterine pathophysiology. Front Endocrinol (Lausanne). 2020; 11: 594370.